Extracting $F_2^{\Lambda}(q^2)/F_2^{\Sigma\Lambda}(q^2)$ from $p(e,e'K^+)\vec{\Lambda}/\vec{\Sigma}^0$ polarizations?

Robert A. Williams* and Toyce Mechelle Small†
Thomas Jefferson National Accelerator Facility, 12000 Jefferson Avenue, Newport News, Virginia 23606
(Received 25 September 1996)

In kaon electroproduction, $p(e,e'K^+)\vec{Y}$ $(Y=\Lambda,\Sigma^0)$, hyperon polarization is an observable which arises from interference between resonant (N^*,Δ^*) and nonresonant amplitudes involving the hyperon anomalous magnetic form factors $F_2^{\Lambda}(q^2)$ and $F_2^{\Sigma\Lambda}(q^2)$. Within the framework of an effective hadronic field Lagrangian model we investigate the possibility suggested by Williams and Truman that the Λ/Σ^0 polarized cross section ratio may be approximately proportional to the form factor ratio $F_2^{\Lambda}/F_2^{\Sigma\Lambda}$ and independent of the dominant N^* amplitude. We illustrate both the simplified case where the relation between the form factor and polarized cross section ratio is an identity and the sensitivity due to dynamical assumptions about nearby resonances and the $g_{KN\Lambda}$ coupling constant. [S0556-2813(97)01502-1]

PACS number(s): 13.40.Gp, 12.40.Vv, 13.88.+e, 14.20.Jn

I. INTRODUCTION

An important emphasis in nuclear physics phenomenology is the development of models based on effective interactions which incorporate dynamic symmetries [e.g., chiral, $SU(3)_F$, crossing, covariance, etc.] to form a unified and consistent description of nuclear structure and reactions. Models which employ symmetries tend to be very efficient (e.g., small number of parameters) and predictive, although sometimes beyond experimental verification. Consider the application of $SU(3)_F$ flavor symmetry in vector meson dominance (VMD) [1,2], quark [3–5], and soliton [6,7] models of octet baryon electromagnetic form factors. In each case, the underlying $SU(3)_F$ symmetry enables a prediction of the hyperon form factors in terms of model parameters fixed by the nucleon data. Theoretical interest in the hyperon form factors centers on understanding the effects of explicit and hidden strangeness on electromagnetic observables. Although it is possible to compare model predictions against lattice QCD calculations [8] (for small spacelike q^2), there is presently no data available for a direct comparison with experiment, except for one timelike measurement of $F_2^{\Lambda}(q^2\approx 5.7\ \mathrm{GeV}^2)$ via $e^+e^-\to\Lambda\bar{\Lambda}$ [9]. There is no obvious way to obtain a spacelike measurement since it is not possible to construct a stable hyperon target. It is natural to question if it is even possible to measure any of the spacelike hyperon form factors by some indirect method. In this paper we address this question by investigating our hypothesis that the polarized $\vec{\Lambda}$ and $\vec{\Sigma}^0$ cross sections near threshold in kaon electroproduction are dominated by interference between the $N^*(1710)$ resonance and Born amplitudes proportional to the Pauli magnetic form factors F_2^{Λ} and $F_2^{\Sigma\Lambda}$, respectively. Our hypothesis is based on model calculations (described later) showing that both Λ and Σ^0 photoproduction polarizations are strongly peaked at the $N^*(1710)$ resonance energy and enhanced for backward (c.m.) kaon production angles (i.e., large $|t|$, small $|u|$ kinematics). This is precisely the energy and angular dependence we expect as a signature for polarization dominated by interference between a resonant s-channel N^* and nonresonant u-channel hyperon amplitude. Since our model has a much larger $KN\Lambda$ coupling compared to $KN\Sigma$ (i.e., $g_{KN\Lambda}\gg g_{KN\Sigma}$), we naively expect the q^2 dependence of polarized Λ (Σ^0) production to be governed by the product of the N^* transition, $F_2^{N^*N}(q^2)$, and anomalous magnetic $F_2^{\Lambda}(q^2)$ $[F_2^{\Sigma\Lambda}(q^2)]$ form factors. To test our hypothesis, we note that the q^2 dependence of the $\vec{\Lambda}/\vec{\Sigma}^0$ polarized cross section ratio should be independent of the common $N^*(1710)N\gamma$ transition form factor. Furthermore, if our hypothesis is correct, then the choice of hyperon form factors should govern the q^2 dependence of the polarized cross section ratio for whatever assumptions we make about the hyperon form factor behavior. We investigate three models of the hyperon form factors exhibiting very different q^2 dependence to test the general validity of our hypothesis.

Before moving on to a discussion of our calculation we note that even if we could unambiguously prove the validity of our proposed technique, experiments following our prescription would be very difficult. Although the $\vec{\Lambda}$ polarization is self-analyzing due to the weak decay $\Lambda\to\pi^-p$, the $\vec{\Sigma}^0$ polarization would be very difficult to measure since it decays nearly 100% by the radiative transition $\Sigma^0\to\Lambda\gamma$. We emphasize that our goal is to test the conceptual feasibility of our hypothesis from a theoretical point of view. We simply acknowledge that there are experimental difficulties which we do not attempt to overcome or address in detail.

II. MODEL DETAILS

A comprehensive theoretical model was previously developed for the electromagnetic production of the low-lying Λ,Σ^0 hyperons [10–12]. The model parameters were determined by a simultaneous fit to the low-energy photoproduction, $p(\gamma,K^+)Y$, electroproduction, $p(e,e'K^+)Y$, and radiative capture, $p(K^-,\gamma)Y$, data in the $Y=\Lambda,\Sigma^0,\Lambda(1405)$ hyperon channels. To simplify our analysis we consider the

*Present address: Hampton University, Department of Physics, Hampton, Virginia 23668. Electronic address: bobw@cebaf.gov
†Present address: Jackson State University, Department of Physics, Jackson, Mississippi 39217.

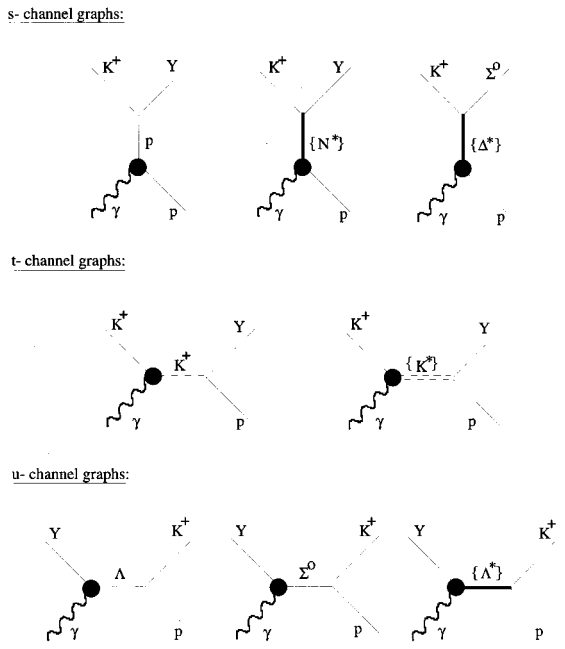

FIG. 1. Feynman diagrams contributing to $p(e,e'K^+)\Lambda,\Sigma^0$ in our model. $\{N^*\}\equiv\{N(1650),\ N(1710)\}$, $\{\Delta^*\}\equiv\{\Delta(1620),\ \Delta(1900),\ \Delta(1910)\}$, $\{\Lambda^*\}\equiv\{\Lambda(1405)\}$. K^* diagrams are excluded as a passive duality constraint.

minimal low-energy model detailed in Ref. [11] which incorporates a passive duality constraint through elimination of t-channel K^* diagrams and a truncation of baryon resonances with spin $\geqslant 3/2$. In Fig. 1 we display the Feynman diagrams and corresponding resonances that detail the dynamical content of our model. We have shown in Ref. [12] that the K^* amplitudes generate higher partial waves required at intermediate energies ($\sqrt{s}\gtrsim 1.9$ GeV) due to our neglect of higher spin baryon resonances, but have a questionable role in the hyperon production mechanism near threshold. We show later that our hyperon polarization hypothesis breaks down even in our minimal model, and thus investigating possible K^* effects becomes a moot point which we do not pursue. We review some of the essential details about the electroproduction formalism in the next section. Additional discussion including expressions for the covariant Feynman amplitudes and numerical values of the effective Born and resonance coupling constants can be found in Ref. [12].

III. ELECTROPRODUCTION FORMALISM

To establish notation for explicit discussion, consider the electroproduction reaction

$$e(e_1)+p(p)\rightarrow e'(e_2)+K^+(k)+Y(l), \tag{1}$$

where each particle's four-momentum is labeled in parentheses. The virtual photon momentum is defined to be $q=e_1-e_2$. In the one-photon-exchange approximation, the transition amplitude for hyperon $Y=\Lambda,\Sigma^0$ production is expressed as the invariant product of leptonic ($\mathcal{L}^{\mu}$) and hadronic ($\mathcal{H}_Y^{\nu}$) currents mediated by the photon propagator $g_{\mu\nu}/q^2$:

$$t_Y=\frac{\mathcal{L}\cdot\mathcal{H}_Y}{q^2}. \tag{2}$$

The unpolarized differential cross section is calculated from the spin-averaged squared transition amplitude

$$\langle|t_Y|^2\rangle=\frac{1}{4}\sum_{s_1,s_2}\sum_{\lambda,\lambda'}|e\overline{u_{e'}}(e_2,s_2)\frac{\gamma_\mu}{q^2}u_e(e_1,s_1)\mathcal{H}_Y^{\mu}(\lambda,\lambda')|^2 \tag{3}$$

$$=\frac{e^2}{4q^4M_e^2}\sum_{\lambda,\lambda'}[\tfrac{1}{2}q^2|\mathcal{H}_Y(\lambda,\lambda')|^2 +2|e_1\cdot\mathcal{H}_Y(\lambda,\lambda')|^2], \tag{4}$$

where for each external spin-1/2 particle carrying four-momentum x and spin projection λ we associate a Dirac spinor $u(x,\lambda)$. The hadronic current is explicitly conserved through the decomposition

$$\mathcal{H}_Y^{\mu}(\lambda,\lambda')=\overline{u_Y}(l,\lambda')\left[\sum_{i=1}^{6}B_i(s,t,q^2)\mathcal{N}_i^{\mu}\right]u_p(p,\lambda). \tag{5}$$

The $B_i(s,t,q^2)$ factors are the so-called invariant (or covariant Feynman) amplitudes, which are scalar functions of the Lorentz-invariant Mandelstam variables, and the $\mathcal{N}_{\mu}^{i}$ terms form a complete basis of gauge-invariant matrices (Dirac operators):

$$N_{\mu}^1=\tfrac{1}{2}\gamma_5(\gamma\cdot q\gamma_\mu-\gamma_\mu\gamma\cdot q),\quad N_{\mu}^2=\gamma_5\left(p_\mu-\frac{p\cdot q}{q^2}q_\mu\right),$$

$$N_{\mu}^3=\gamma_5\left(l_\mu-\frac{l\cdot q}{q^2}q_\mu\right),\quad N_{\mu}^4=\gamma_5(p\cdot q\gamma_\mu-\gamma\cdot qp_\mu),$$

$$N_{\mu}^5=\gamma_5(l\cdot q\gamma_\mu-\gamma\cdot ql_\mu),\quad N_{\mu}^6=\gamma_5(\gamma\cdot qq_\mu-q^2\gamma_\mu). \tag{6}$$

The polarization of the final-state hyperon is defined as the asymmetry in the differential cross section between spin-up and spin-down hyperon production. We employed a covariant spin projection operator to determine the spin-up and spin-down hadronic current,

$$\Pi(\uparrow\downarrow)=\tfrac{1}{2}(1\pm\gamma_5\gamma\cdot\xi). \tag{7}$$

ξ_μ is a spacelike unit-4 vector perpendicular to the hyperon momentum direction ($l\cdot\xi=0$) which defines the spin quantization axis, taken to be normal to the hadronic scattering plane defined in Ref. [12] (spin ''up'' corresponds to the direction $\hat{y}=\hat{q}\times\hat{k}$):

$$\xi_\mu=(0,\ -\sin\phi,\ \cos\phi,\ 0), \tag{8}$$

where ϕ is the angle between leptonic and hadronic scattering planes. The polarized hadronic current is

$$\mathcal{H}_Y^{\mu}(\uparrow\downarrow)=\overline{u_Y}(l,\lambda')\overline{\Pi}(\uparrow\downarrow)\left[\sum_{i=1}^{6}B_i(s,t,q^2)\mathcal{N}_i^{\mu}\right]u_p(p,\lambda), \tag{9}$$

where

$$\overline{\Pi}(\uparrow\downarrow)=\gamma_0\Pi^\dagger(\uparrow\downarrow)\gamma_0=\Pi(\downarrow\uparrow). \tag{10}$$

In this analysis, we calculate only the transverse two-body virtual photoproduction cross sections, which assume a particularly simple form in the c.m. system and permit a direct comparison with photoproduction (i.e., $q^2\to 0$):

$$d\sigma_Y(\uparrow\downarrow)\equiv\frac{d\sigma_Y^{\text{c.m.}}}{d\Omega_K}(\uparrow\downarrow)$$
$$=\frac{|\mathbf{k}|}{|\mathbf{q}|}\frac{M_pM_Y}{16\pi^2 s}\sum_{\lambda,\lambda'}\tfrac{1}{2}[|\mathcal{H}_Y^x(\uparrow\downarrow)|^2+|\mathcal{H}_Y^y(\uparrow\downarrow)|^2]. \tag{11}$$

The unpolarized (polarized) differential cross sections are obtained from the definitions

$$d\sigma_Y=d\sigma_Y(\uparrow)+d\sigma_Y(\downarrow), \tag{12}$$

$$\mathcal{P}_Y d\sigma_Y=d\sigma_Y(\uparrow)-d\sigma_Y(\downarrow), \tag{13}$$

where $\mathcal{P}_Y$ is the polarization of the $Y=\Lambda,\Sigma^0$ hyperon.

To demonstrate that the hyperon polarization is an interference observable, we consider the covariant expressions for the spin-projected squared transition amplitude. Using the spinor completeness relation $\Sigma_\lambda u(x,\lambda)\overline{u(x,\lambda)}=(\gamma\cdot x+M_x)/2M_x$, and defining the usual electromagnetic fine structure constant ($\alpha_e=e^2/4\pi$), the squared spin-projected transition amplitude can be expressed as

$$|t_Y(\uparrow\downarrow)|^2=\left(\frac{\pi\alpha_e}{8M_YM_pM_e^2}\right)\left(\frac{1}{q^2}\right)\sum_{i,j=1}^{6}B_iB_j^*[T_1^{ij}(\uparrow\downarrow)+T_2^{ij}(\uparrow\downarrow)], \tag{14}$$

with

$$T_1^{ij}(\uparrow\downarrow)\equiv\text{Tr}[(\gamma\cdot l+M_Y)\overline{\Pi}(\uparrow\downarrow)\mathcal{N}_\mu^i(\gamma\cdot p+M_p)\overline{\mathcal{N}_\nu^j}g^{\mu\nu}]. \tag{15}$$

Here we consider only the T_1^{ij} sum in Eq. (14) which corresponds to the polarized photoproduction cross section when $q^2\to 0$. Note that all of the nonzero terms in the trace formula (15) coming from the first term of the projection operator are purely real and correspond to 1/2 of the unpolarized cross section, whereas from the second term (involving $\pm\frac{1}{2}\gamma_5\gamma\cdot\xi$) there is a common factor

$$\pm\text{Tr}[(\gamma\cdot l)(\gamma\cdot p)(\gamma\cdot q)(\gamma\cdot\xi)\gamma_5]=\pm 4i\epsilon^{\mu\nu\alpha\beta}l_\mu p_\nu q_\alpha\xi_\beta \tag{16}$$

$$\overset{\text{c.m.}}{\to}\pm 4i\sqrt{s}|\mathbf{k}||\mathbf{q}|\sin\theta_{\text{c.m.}}, \tag{17}$$

which is purely imaginary and determines the polarized cross section. Also note that the polarization angular distribution has an overall $\sin\theta_{\text{c.m.}}$ dependence (θ is the angle between the photon and kaon) and thus vanishes for extreme forward and backward c.m. kaon angles. The polarized cross section has the form

TABLE I. Effective vector meson coupling constants of the three hyperon form factor models.

	$\kappa_V C_V$		
V	I	II	III
ρ	$-0.5\kappa_{\Sigma\Lambda}$	$\kappa_{\Sigma\Lambda}$	$-3.3\kappa_{\Sigma\Lambda}$
ω	$0.5\kappa_\Lambda$	0	0
ϕ	$0.5\kappa_\Lambda$	κ_Λ	$1.6\kappa_\Lambda$

$$\mathcal{P}_Y d\sigma_Y\equiv K_Y(|t_Y(\uparrow)|^2-|t_Y(\downarrow)|^2) \tag{18}$$

$$=K_Y'\sum_{i,j=1}^{6}\text{Im}(B_iB_j^*)\text{Im}(T_1^{ij}), \tag{19}$$

where K_Y and K_Y' are overall kinematic factors which depend on the hyperon mass. Here we see the interference structure of the polarized hyperon cross section in the bilinear product $\text{Im}(B_iB_j^*)$. We employ resonance propagators of the form $(s-M_{N*}^2+iM_{N*}\Gamma_{N*})^{-1}$, and hence for energies corresponding to a narrow s-channel resonance (i.e., $\sqrt{s}=M_{N*}$) the polarized cross section is dominated by the product of purely imaginary resonance and purely real background amplitudes. Our goal is to establish whether or not the real amplitudes are primarily the Born terms proportional to the unknown hyperon form factors.

IV. MODEL FORM FACTORS

Hadronic substructure is accommodated through the use of extended vector meson dominance electromagnetic form factors [1,13]. The nonstrange baryon resonance transition form factors are assumed to be proportional to $F_2^p(q^2)$ of the proton. We parametrize the hyperon form factors with the functional form

$$\kappa_\Lambda F_2^\Lambda(q^2)=F_2^\gamma(q^2)\left[\kappa_\Lambda+\kappa_\omega C_\omega\frac{q^2}{M_\omega^2-q^2}+\kappa_\phi C_\phi\frac{q^2}{M_\phi^2-q^2}\right], \tag{20}$$

$$\kappa_{\Sigma\Lambda}F_2^{\Sigma\Lambda}(q^2)=F_2^\gamma(q^2)\left[\kappa_{\Sigma\Lambda}+\kappa_\rho C_\rho\frac{q^2}{M_\rho^2-q^2}\right]. \tag{21}$$

The $F_2^\gamma(q^2)$ function interpolates the small q^2 behavior governed by the vector meson poles to the large q^2 behavior governed by perturbative QCD [1]. We use the experimental values for the anomalous magnetic moments $\kappa_\Lambda=-0.61$ and $\kappa_{\Sigma\Lambda}=1.61$. The effective vector meson coefficients κ_VC_V are chosen in three models to produce distinct q^2 behavior for the $F_2^\Lambda/F_2^{\Sigma\Lambda}$ form factor ratio. Numerical values of the coefficients are listed in Table I. Model I produces a decreasing form factor ratio with increasing q^2, whereas models II and III have increasing ratios. Model I corresponds to an arbitrary choice which we used in our preliminary analysis reported in Ref. [1]. Model II is a special limit that reduces the Λ form factor (20) to a simple product of ω and ϕ poles (at low $|q^2|$) and the $\Sigma\Lambda$ transition form factor (21) to a second-order ρ pole. Model III employs couplings derived

from the universality relations of our baryon octet model [1]. We use the F_2^{Λ} parameters from our previous work, but the $\Sigma\Lambda$ form factor (which is a $\Delta I=1$ transition) requires a simple extension to our universality relations using Clebsch-Gordon coefficients:

$$C_\rho(\Sigma^0\Lambda)=\frac{(1100|00)}{(1101|11)}C_\rho(\Sigma^+)=\sqrt{\tfrac{2}{3}}C_\rho(\Sigma^+). \quad (22)$$

Before we discuss numerical results, we illustrate a toy calculation showing the limits when the polarized cross section and form factor ratios are approximately and exactly proportional.

V. TOY CALCULATION OF $\mathcal{P}_Y d\sigma_Y$

Starting from Eq. (19), we note that each invariant amplitude B_i gets contributions from each hadronic field in the space of our model (although some terms are zero). If we dial the energy corresponding to a narrow, $I=1/2$ nucleon resonance (i.e., $\sqrt{s}=M_{N^*}$), then we can make the decomposition

$$B_i=B_i^b+B_i^{\Lambda}+iB_i^{N^*}, \quad (23)$$

where B_i^b represents all of the real background amplitudes other than the Λ [i.e., p, K^+, Σ^0, $\Lambda(1405)$, ...], and we assume strong dominance of the single N^* resonance for the imaginary component. The Λ field is singled out because it is weighted with a relatively large coupling constant and we assume some enhancement at backward kaon angles (coming from its propagator) relative to the other real amplitudes. Now we re-express Eq. (19) in the form

$$\mathcal{P}_Y d\sigma_Y=K_Y'\sum_{ij}\ \mathrm{Im}(T_1^{ij})\{[B_i^{N^*}B_j^{\Lambda}-B_j^{N^*}B_i^{\Lambda}] +[B_i^{N^*}B_j^{b}-B_j^{N^*}B_i^{b}]\}. \quad (24)$$

In the limit when the B_i^b amplitudes are negligible compared with those of the Λ (i.e. if $B_i^{\Lambda}\gg B_i^b$), there is pure interference between the N^* and Λ amplitudes. Now we consider the form of the invariant amplitudes for hyperon $Y=\Lambda,\Sigma^0$ production:

$$B_i^{\Lambda}(Y)=g_{KN\Lambda}\frac{\mu_{Y\Lambda}F_2^{Y\Lambda}}{u-M_{\Lambda}^2}C_i(Y), \quad (25)$$

$$B_i^{N^*}(\Sigma)=\left(\frac{g_{KN^*\Sigma}}{g_{KN^*\Lambda}}\right)B_i^{N^*}(\Lambda), \quad (26)$$

where the $C_i(Y)$ factors are constants that depend on the hyperon mass [e.g., $C_1(\Lambda)=2M_{\Lambda}$; $C_1(\Sigma)=M_{\Lambda}+M_{\Sigma}$], and the N^* amplitudes for Σ^0 versus Λ production differ by a constant. Note that the Λ and Σ^0 have the same spin, parity, and nearly the same mass; therefore, the $C_i(\Sigma)$ and $C_i(\Lambda)$ factors all have the same signs and differ by the small Σ-Λ mass difference. Setting $C_i(\Sigma)\approx C_i(\Lambda)\equiv C_i$, $K_{\Sigma}'\approx K_{\Lambda}'$, $B_i^{N^*}(\Lambda)\equiv B_i^{N^*}$, and taking the Λ/Σ^0 polarized cross section ratio, we obtain

$$\frac{\mathcal{P}_{\Lambda}d\sigma_{\Lambda}}{\mathcal{P}_{\Sigma}d\sigma_{\Sigma}}\approx\frac{K_{\Lambda}'g_{KN\Lambda}[\mu_{\Lambda}F_2^{\Lambda}(q^2)/(u-M_{\Lambda}^2)]}{K_{\Sigma}'g_{KN\Lambda}[\mu_{\Sigma\Lambda}F_2^{\Sigma\Lambda}(q^2)/(u-M_{\Lambda}^2)](g_{KN^*\Sigma}/g_{KN^*\Lambda})}\ \frac{\Sigma_{ij}[B_i^{N^*}C_j-B_j^{N^*}C_i]}{\Sigma_{ij}[B_i^{N^*}C_j-B_j^{N^*}C_i]}, \quad (27)$$

$$=\left(\frac{\mu_{\Lambda}}{\mu_{\Sigma\Lambda}}\frac{g_{KN^*\Lambda}}{g_{KN^*\Sigma}}\right)\frac{F_2^{\Lambda}(q^2)}{F_2^{\Sigma\Lambda}(q^2)}. \quad (28)$$

Therefore, under the assumptions of pure N^*-Λ interference and equal-mass hyperons, we see that the polarized cross section ratio q^2 dependence is proportional to the hyperon form factor ratio and independent of the $N^*p\gamma$ transition form factor. In the next section we investigate numerical sensitivity to the Σ-Λ mass difference and specific dynamical assumptions about our amplitudes. We find that the Σ-Λ mass difference effect can be minimized with respect to the c.m. kaon angle, but our simplifying dynamical approximations made in deriving Eq. (28) (i.e., neglect of interference with other Born and resonance background terms) are not valid in our full electroproduction model.

VI. NUMERICAL RESULTS

In Figs. 2–4 we show the results from our preliminary analysis, qualitatively discussed in Ref. [1], which led us to this more detailed investigation. In Fig. 2 we plot the energy dependence of the Λ and Σ^0 photoproduction ($q^2=0$) polarizations of our full model (i.e., no approximations). Note the strong $N^*(1710)$ resonance peaks for both Σ^0 and Λ polarization. Also note that the peak Σ^0 polarization is larger than the Λ, which appears to be consistent with pure interference between the $N^*(1710)$ and Λ amplitudes, since the product of effective $\Sigma\Lambda$ and $N^*(1710)$ couplings is larger than the product of Λ and $N^*(1710)$ couplings, $(\mu_{\Sigma\Lambda}g_{KN\Lambda})(\mu_{N^*p}g_{KN^*\Sigma}) > (\mu_{\Lambda}g_{KN\Lambda})(\mu_{N^*p}g_{KN^*\Sigma})$. The Σ^0 also gets a large polarization from Δ resonances for energies above $\sqrt{s}\gtrsim 1.85$ GeV, but decouple from the Λ due to isospin conservation. In Fig. 3 we show the corresponding polarization angular distributions, which vanish at the end points (as expected) and show a backward angle enhancement for both Λ and Σ^0, consistent with the idea that the dominant interference from the real background is due to Λ propagation. Figure 4 displays the q^2 dependence of the hyperon form factor (model I) and polarized cross section ratio (normalized at the photoproduction point) for two dif-

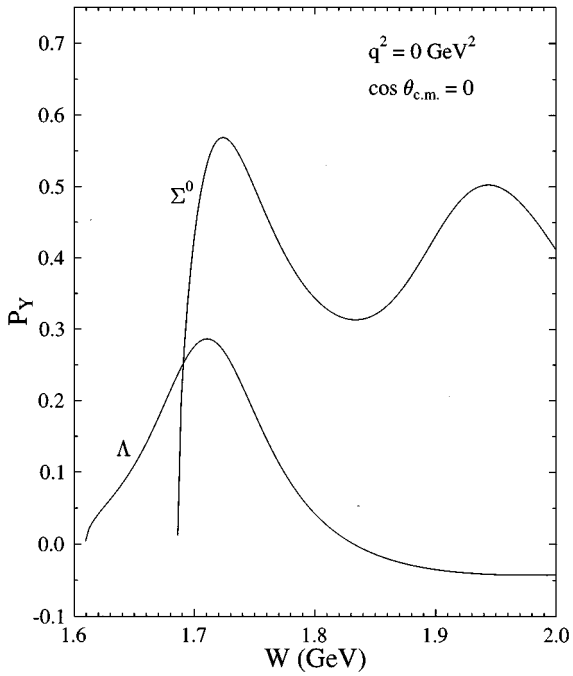

FIG. 2. Photoproduction energy dependence of the hyperon polarizations.

ferent c.m. kaon angles. Note the dramatic improvement of the polarized cross section ratio at a backward kaon angle ($\cos\theta_{\text{c.m.}} = -0.85$) in following the hyperon form factor ratio, which is intuitively consistent with our hypothesis that the Λ and Σ^0 polarizations (near threshold) are dominated by pure interference between the $N^*(1710)$ and Λ amplitudes. Although these preliminary results seem to support our hypothesis and suggest a possible method for measuring the

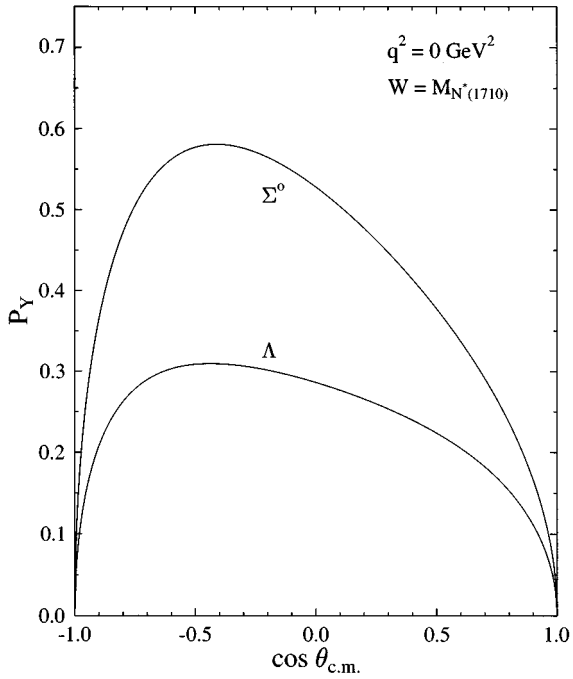

FIG. 3. Photoproduction angular dependence of the hyperon polarizations.

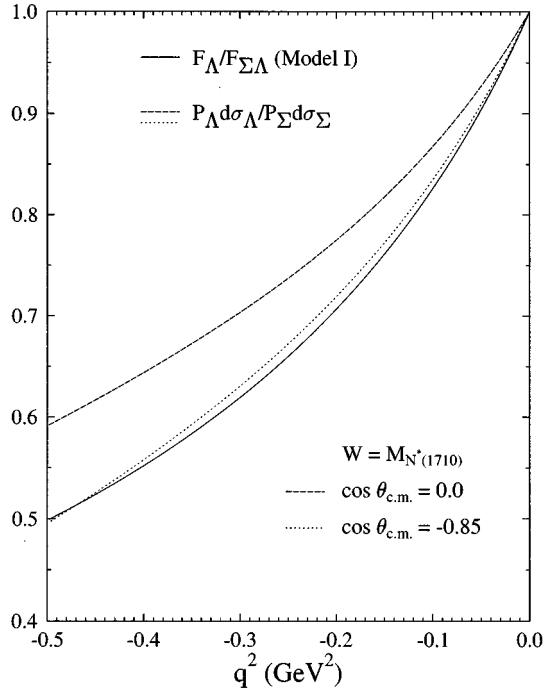

FIG. 4. Polarized cross section ratio (normalized to photoproduction) $d\sigma_\Lambda \mathcal{P}_\Lambda / d\sigma_\Sigma \mathcal{P}_\Sigma$ compared with the model I hyperon form factor ratio $F_2^\Lambda / F_2^{\Sigma\Lambda}$ as a function of q^2.

spacelike hyperon form factor ratio, we now show that upon closer examination our original interpretation was incorrect or, at least, oversimplified.

In order to understand deviations of our hypothesis coming from the Σ-Λ mass difference independently from specific dynamical approximations, we now discuss the numerical results of our toy polarization model [i.e., pure interference between $N^*(1710)$ and Λ]. In Figs. 5–7, we plot the polarized cross section and hyperon form factor ratios of models I, II, and III for $\cos\theta_{\text{c.m.}} = -0.85$, 0.0, and 0.85, respectively. We find that the Σ-Λ mass difference has a minimum effect for $\cos\theta_{\text{c.m.}} \approx 0$, as seen in Fig. 6. We have verified numerically that if we artificially set $M_\Sigma = M_\Lambda$ in our program, then our toy calculation reproduces the identity (28) for any choice of $\cos\theta_{\text{c.m.}}$. In the remaining figures we fix $\cos\theta_{\text{c.m.}} = 0.0$, so that any deviation of the polarized cross section ratio from the hyperon form factor ratio can be attributed to dynamical effects.

In Figs. 8–10 we show the q^2 dependence of models I, II, and III, respectively, compared with the polarized cross section ratios. Here we see a breakdown of our hypothesis since the degree to which the polarized cross section ratio follows the form factor ratio depends on the choice of form factor model. The comparison gets progressively worse going from model I to III. In each figure we also show the sensitivity of our results to the input $g_{KN\Lambda}$ coupling constant. From the toy calculation, Eqs. (27) and (28), we know that the polarized cross section ratio should be independent of $g_{KN\Lambda}$ if our original hypothesis [i.e., pure $N^*(1710)$-Λ interference] were correct. Our results suggest that interference terms other than pure N^*-Λ are important and violate the dynamical approximations leading to Eq. (28).

To further understand the breakdown of our hypothesis,

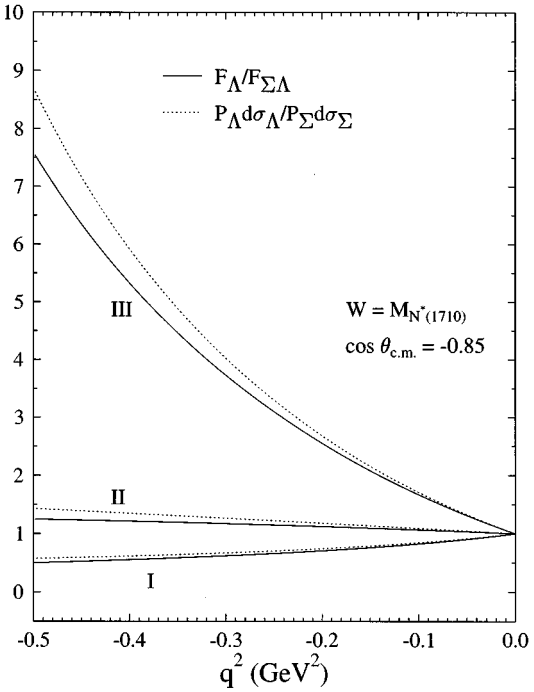

FIG. 5. Toy model polarized cross section ratio (normalized to photoproduction) $d\sigma_\Lambda \mathcal{P}_\Lambda / d\sigma_\Sigma \mathcal{P}_\Sigma$ compared with the models I, II, and III hyperon form factor ratios $F_2^{\Lambda}/F_2^{\Sigma\Lambda}$ as a function of q^2 for $\cos\theta_{\text{c.m.}} = -0.85$.

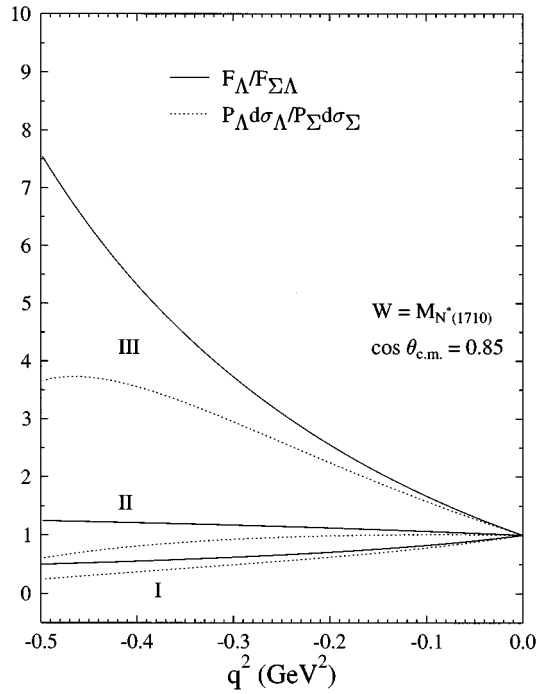

FIG. 7. Toy model polarized cross section ratio (normalized to photoproduction) $d\sigma_\Lambda \mathcal{P}_\Lambda / d\sigma_\Sigma \mathcal{P}_\Sigma$ compared with the models I, II, and III hyperon form factor ratios $F_2^{\Lambda}/F_2^{\Sigma\Lambda}$ as a function of q^2 for $\cos\theta_{\text{c.m.}} = 0.85$.

we investigate polarization contributions arising from individual interference terms in our model space. In Figs. 11 and 12 we plot the energy dependence of the polarized $\vec{\Lambda}$ and $\vec{\Sigma}^0$ cross sections, respectively, for various interference combinations. In both figures the solid line is the full calculation and the dotted line represents the full result without $N^*(1710)$-Λ interference, whereas the dashed line corresponds to pure $N^*(1710)$-Λ interference. We see that the

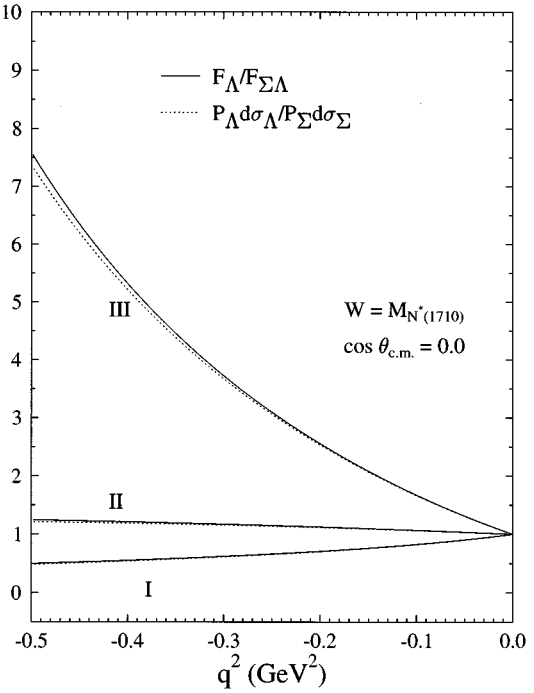

FIG. 6. Toy model polarized cross section ratio (normalized to photoproduction) $d\sigma_\Lambda \mathcal{P}_\Lambda / d\sigma_\Sigma \mathcal{P}_\Sigma$ compared with the models I, II, and III hyperon form factor ratios $F_2^{\Lambda}/F_2^{\Sigma\Lambda}$ as a function of q^2 for $\cos\theta_{\text{c.m.}} = 0.0$.

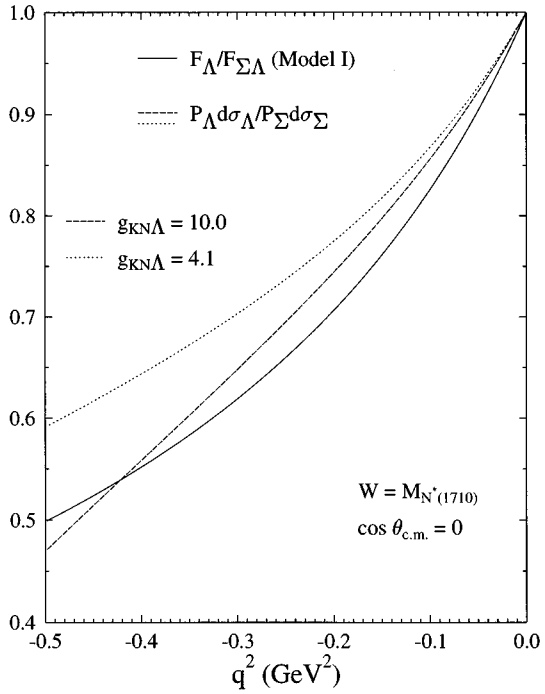

FIG. 8. Full calculation of the polarized cross section ratio using model I hyperon form factors, showing sensitivity to the $g_{KN\Lambda}$ coupling constant.

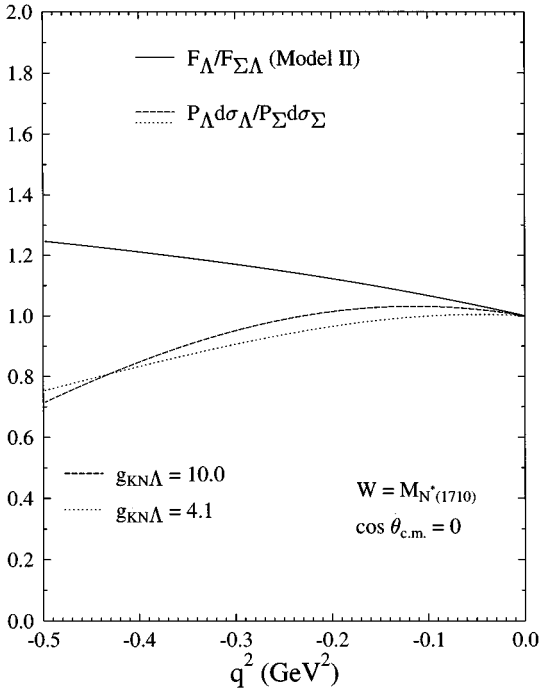

FIG. 9. Full calculation of the polarized cross section ratio using model II hyperon form factors, showing sensitivity to the $g_{KN\Lambda}$ coupling constant.

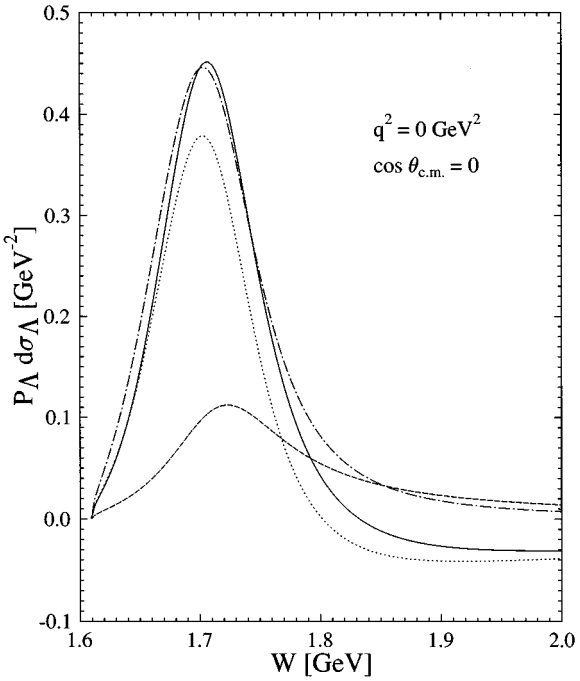

FIG. 11. Energy dependence of the polarized Λ photoproduction cross section for different interference contributions: full calculation (solid line), full calculation with no $N^*(1710)$-Λ interference (dotted line), pure $N^*(1710)$-Λ interference (dashed line), and pure $N^*(1710)$-$N^*(1650)$ interference (dot-dashed line).

$\vec{\Sigma}^0$ polarization is largely dominated by pure $N^*(1710)$-Λ interference (near threshold), but the $\vec{\Lambda}$ polarization gets a much smaller contribution. We find that the dominant mechanism of polarized $\vec{\Lambda}$ photoproduction (in our model) is due to interference between $N^*(1710)$-$N^*(1650)$ resonances, shown as the dot-dashed line in Fig. 11. A key observation is that the $N^*(1650)$ resonance has a mass below the $K^+\Sigma^0$ threshold and above the $K^+\Lambda$ threshold, and thus largely decouples from polarized $\vec{\Sigma}^0$ production, but contrib-

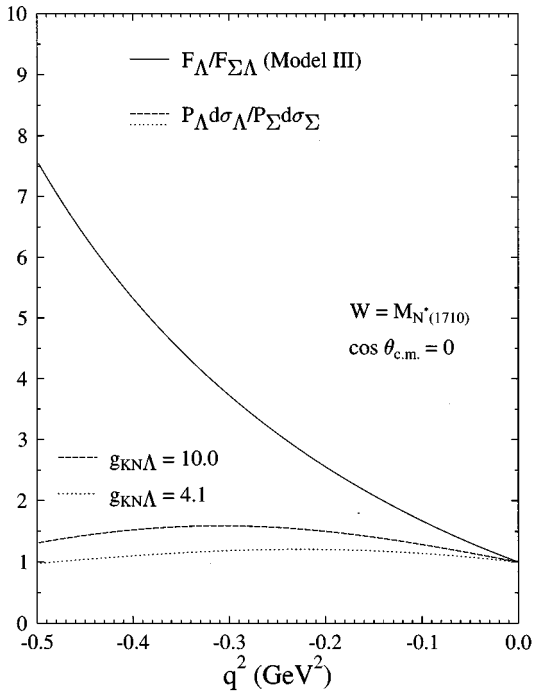

FIG. 10. Full calculation of the polarized cross section ratio using model III hyperon form factors, showing sensitivity to the $g_{KN\Lambda}$ coupling constant.

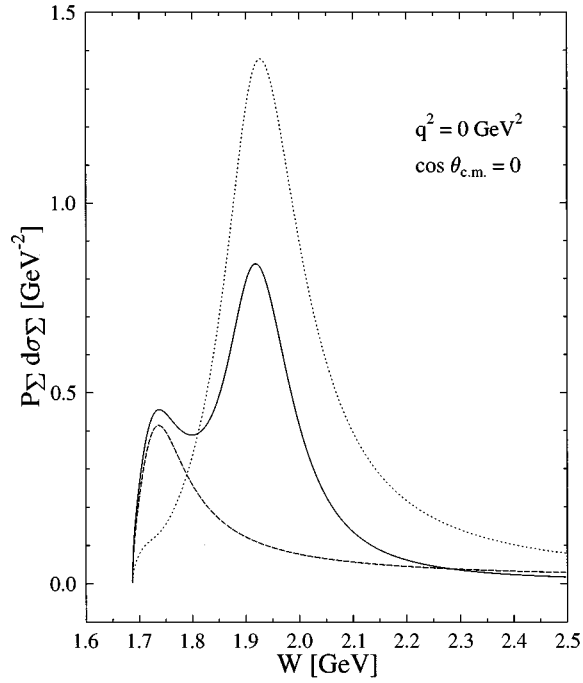

FIG. 12. Energy dependence of the polarized Σ^0 photoproduction cross section for different interference contributions: full calculation (solid line), full calculation with no $N^*(1710)$-Λ interference (dotted line), and pure $N^*(1710)$-Λ interference (dashed line).

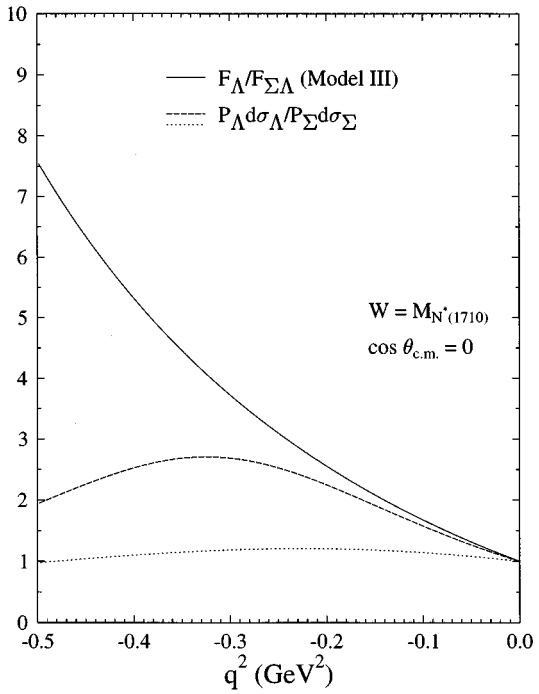

FIG. 13. Sensitivity of the polarized cross section ratio $d\sigma_\Lambda \mathcal{P}_\Lambda / d\sigma_\Sigma \mathcal{P}_\Sigma$ to the $N^*(1650)$ amplitude using the model III hyperon form factors. Dotted line is full calculation and dashed line is calculation with $N^*(1650)$ coupling set to zero.

utes strongly to $\vec{\Lambda}$ polarization. To demonstrate the effect of the $N^*(1650)$ on the polarized cross section ratio, we use the form factor model III, which produces the largest (obvious) violation of the identity (28), and show in Fig. 13 the results of the full calculation consecutively with (dotted line) and without (dashed line) the $N^*(1650)$ contribution. We find that neglecting the $N^*(1650)$ produces close agreement between the form factor and polarized cross section ratio for small q^2, but a growing violation for $|q^2| \gtrsim 0.3$ GeV^2 indicates a transition away from pure $N^*(1710)$-Λ interference.

VII. CONCLUSIONS

Based on qualitative features (i.e., characteristic energy and angular distributions consistent with pure N^*-Λ interference) previously observed in model calculations of $p(\gamma,K^+)\vec{\Lambda}$ and $p(\gamma,K^+)\vec{\Sigma}^0$ polarizations, we proposed a possible method for extracting the $F_2^{\Lambda}/F_2^{\Sigma\Lambda}$ hyperon form factor ratio [1]. Here we have presented a quantitative description of our preliminary results in addition to a detailed analysis of our hypothesis using a phenomenological, low-energy hadronic Lagrangian pole model [12]. Explicit consideration of a toy calculation based on pure N^*-Λ interference has helped to clarify the role of dynamical approximations and the presence of effects coming from the Σ-Λ mass difference while providing a benchmark for testing our hypothesis. We have shown that the q^2 behavior of the polarized hyperon cross section ratio is very sensitive to dynamical assumptions about nearby resonances [e.g., $N^*(1650)$ amplitude]. We conclude that our suggested technique for extracting the hyperon form factor ratio is not valid in this model and is not likely to be valid in any model unless there is nearly pure N^*-Λ interference for both $\vec{\Lambda}$ and $\vec{\Sigma}^0$ production mechanisms. In passing, we note that since our model predicts nearly pure $N^*(1710)$-Λ interference for $\vec{\Sigma}^0$ polarization, the q^2 dependence of the peak polarized cross section near $\sqrt{s} = 1.71$ GeV is approximately proportional to the product of $N^*(1710)p\gamma$ and $\Sigma\Lambda\gamma$ transition form factors. Although this possibilty is interesting, one should be careful to understand the effects of nearby spin-3/2 resonances such as $N^*(1700;3/2^-)$ and $N^*(1720;3/2^+)$ before suggesting a viable experiment.

ACKNOWLEDGMENTS

The authors thank Hampton University's NuHEP director Warren Buck and outreach coordinator Carlane Pittman for their support of the UnIPhy undergraduate summer research program. R.A.W. acknowledges support from NSF Grant No. HRD-9633750.

[1] R. A. Williams and C. P. Truman, Phys. Rev. C **53**, 1587 (1996).
[2] S. Dubnicka, A. Z. Dubnickova, J. Kraskiewicz, and R. Raczka, Z. Phys. C **68**, 153 (1995).
[3] H.-C. Kim, A. Blotz, M.V. Polyakov, and K. Goeke, Report No. hep-ph/9504363, 1995; Phys. Rev. D **53**, 4013 (1996).
[4] J. P. Kroll, M. Schuermann, and W. Shweiger, Z. Phys. A **347**, 109 (1993).
[5] M. Warns, W. Pfeil, and H. Rollnik, Phys. Lett. B **258**, 431 (1991).
[6] C. V. Christov, A. Blotz, H.-C. Kim, P. Pobylitsa, T. Watabe, T. Meissner, E. R. Arriola, and K. Goeke, Prog. Part. Nucl. Phys. **37**, 91 (1996); Report No. RUB-TPII-32/95, 1995.
[7] P. O. Mazur, M. A. Nowak, and M. Praszalowicz, Phys. Lett. **147B**, 137 (1984).
[8] D. B. Leinweber, R. M. Woloshyn, and T. Drapper, Phys. Rev. D **43**, 1659 (1991).
[9] D. Bisello *et al.*, Z. Phys. C **48**, 23 (1990).
[10] R. A. Williams, Ph.D. thesis, North Carolina State University, 1993.
[11] R. A. Williams, C. R. Ji, and S. R. Cotanch, Phys. Rev. C **43**, 452 (1991).
[12] R. A. Williams, C. R. Ji, and S. R. Cotanch, Phys. Rev. C **46**, 1617 (1992).
[13] R. A. Williams, S. Krewald, and K. Linen, Phys. Rev. C **51**, 566 (1995).